



Neutron Science and Technology Group (P-23)

Robert D. Fulton, Group Leader

Constantine (Gus) Sinnis, Dep. Group Leader

Steve Elliott, Acting Dep. Group Leader

Office: (505) 667-5005

Fax: (505) 665-4121

To/MS: See attached distribution list

From/MS: Michael Furlanetto, P-23, MS H803

Phone/Fax: 667-2128/ 665-4121

E-mail: mfurlanetto@lanl.gov

Symbol: P-23:06-32

Date: July 5, 2006

SUBJECT: A NEW METHOD OF PHOTON DOPPLER VELOCIMETRY DATA ANALYSIS APPLIED TO EXPLOSIVELY-DRIVEN SHOCKS IN TIN, MOLYBDENUM, AND BASALT

This memorandum reports some of the results from a recent experimental campaign studying explosively-driven shocks in tin, molybdenum, and basalt. A new method for analyzing photon Doppler velocimetry data is presented; this method avoids the tradeoff in time and frequency resolution inherent to FFT-based methods, albeit at the cost of significantly greater computation time. Also, a summary of our results for the peak stresses generated in tin as a function of sample thickness are presented as a guide for future experiments.

I. The Experimental Campaign

This memorandum reports some of the results of an experimental campaign undertaken at the Bechtel Nevada Special Technologies Laboratory (BN/STL) in Goleta, California from May 18 to June 2, 2006. The experiments were a collaboration between myself, Mark Wilke, Steve Jaramillo, and Andrew Montoya of P-23, Achim Seifert of P-24, and Dale Turley, Jerry Stevens, Lynn Veaser, and Mike Grover of Bechtel Nevada. Adam Iverson of Bechtel Nevada's Los Alamos Operations facility (BN/LAO) provided hardware and support for the PDV system, and Sarah Giandoni of BN/LAO provided a PDV data analysis program. We used the explosives facility at BN/STL to drive shocks into small samples of material and observed the results.

These experiments were designed to answer several questions:

1. How do surface features, especially the overall surface roughness, change as a material is shocked to a partially molten release state? This was addressed by two shots on tin in which high-magnification visible images were recorded. One shot used Detasheet as an explosive, leaving the tin in a solid state upon release, and the other used PBX 9501 to shock the tin to a partially molten state.

2. What is the distribution of temperatures on the free surface of shocked tin as it goes through the melting-on-release transition? These experiments – a series of eight shots on tin of various thicknesses – built upon a previous campaign by Seifert *et al.* which used multiwavelength

pyrometry to measure a single free surface temperature over a small region. In these experiments we used an infrared camera to measure the variations in temperature across the samples.

3. What are the distributions of temperatures on the free surfaces of shocked molybdenum and basalt? These experiments extended work done by Seifter *et al.* in collaboration with Sarah Stewart-Mukhopadhyay of Harvard University, and were performed in the same manner as the tin experiments.

In order to interpret the results of these experiments, the peak stresses experienced by the samples needed to be known. Previous work showed that VISAR was unable to measure free surface velocities (and thus pressures) once tin began to melt, so on these experiments we fielded a photon Doppler velocimetry (PDV) system. The results obtained from that system are discussed further below.

II. Analysis of PDV Data

PDV has been developed into a standard diagnostic by the efforts of Ted Strand (LLNL) and David Holtkamp (P-22). Our implementation was based on their work and engineering design provided by BN/LAO. Briefly, a 1550 nm DFB-pumped EDFA laser was coupled into a single-mode fiber. Approximately one percent of the light was split off and reflected backward to the detector. The balance of the light exited a bare fiber probe and was reflected off of the target surface from a standoff of 5 to 15 mm. Any motion of the target – such as that caused by an explosively-driven shock – caused the frequency of the reflected light to change. This light was recombined with the unshifted reference beam and directed to a high-bandwidth detector. The two beams beat against each other, and the detector measured these beats directly.

In their raw form, PDV data are simply a record of light intensity at the detector as a function of time. A typical example is shown below in Figure 1. (These data will be used as an example throughout this section. They were taken from an experiment involving a 1.56 mm thick molybdenum target being shocked by PBX 9501. None of the conclusions which follow depend on the particulars of the example.) Typically, PDV data are analyzed by a sliding fast Fourier transform (FFT), which is a three step process:

1. A number of points are chosen for analysis and pre-processed. This procedure usually consists of convolving the points with a window function to suppress unwanted frequency components, though the same effect could be achieved by frequency-domain filtering.
2. The signal within this region is converted to frequency space by a Fourier transform and plotted in a spectrogram.
3. The chosen region is moved a certain number of points along the data, and the process is repeated.

The results of this procedure are shown in Figure 2. A small precursor wave is visible just before shock breakout. Velocity pullback from spallation and the subsequent ringing are then seen, as well as a reacceleration of the surface, most likely from further interaction with the explosive gases. The surface impacts the probe at approximately 5 μ s on the scale used in Figure 2.

Figure 1

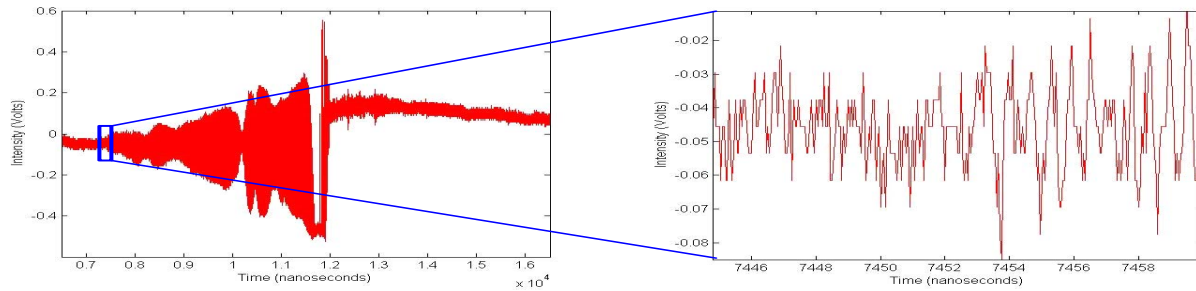


Figure 1: Typical raw PDV data. The plot on the left shows the raw data from 6.5 μ s to 16.5 μ s after the detonator was activated. The plot on the right expands the scale around the time when shock breakout occurred; the increase in intensity and clear pattern of oscillations are both indicative of shock breakout.

Figure 2

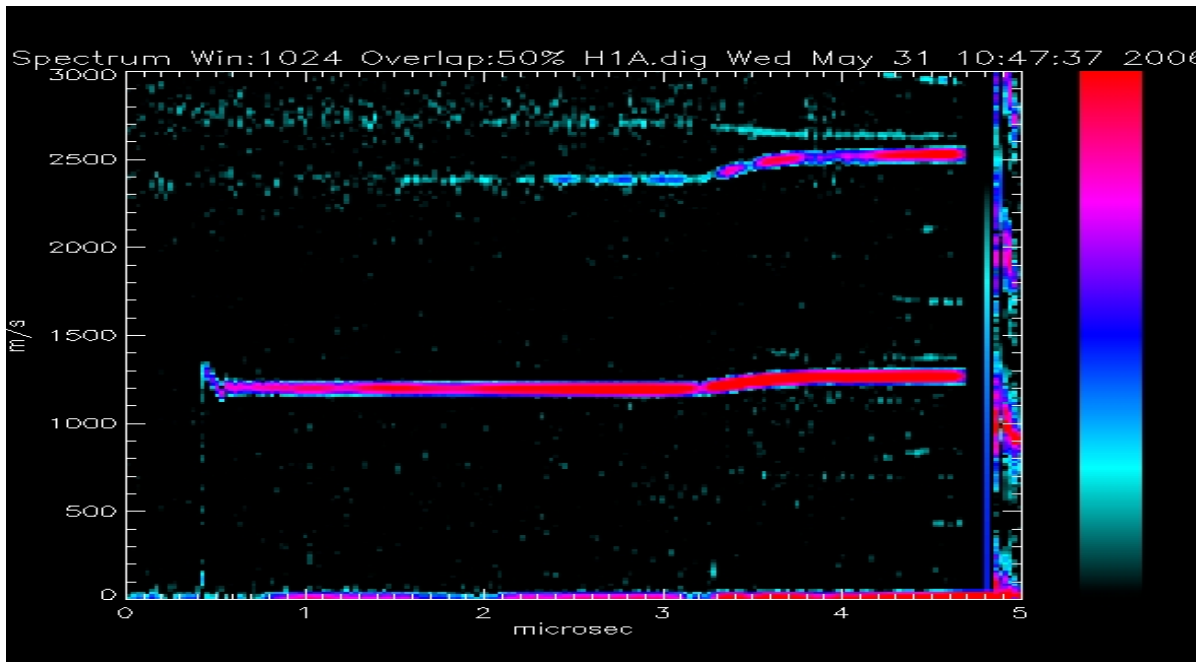


Figure 2: Typical PDV Spectrogram. The velocity is plotted as a function of time after triggering the PDV system; this time is 7 μ s after the detonator fired. Intensities range from -76 dB to -36 dB. The FFT was done over 1024 points at a time after convolution with a Blackman-Harris window, and the increment between transformations was 512 points. The features in the spectrogram above 2000 m/s are harmonics generated in the detector. This plot, as well as the ones in Figure 3, was generated with the PDV program written by Sarah Giandoni of BN/LAO¹.

¹ For further information, contact Fred Sanders at sanderf@nv.doe.gov.

Figure 3

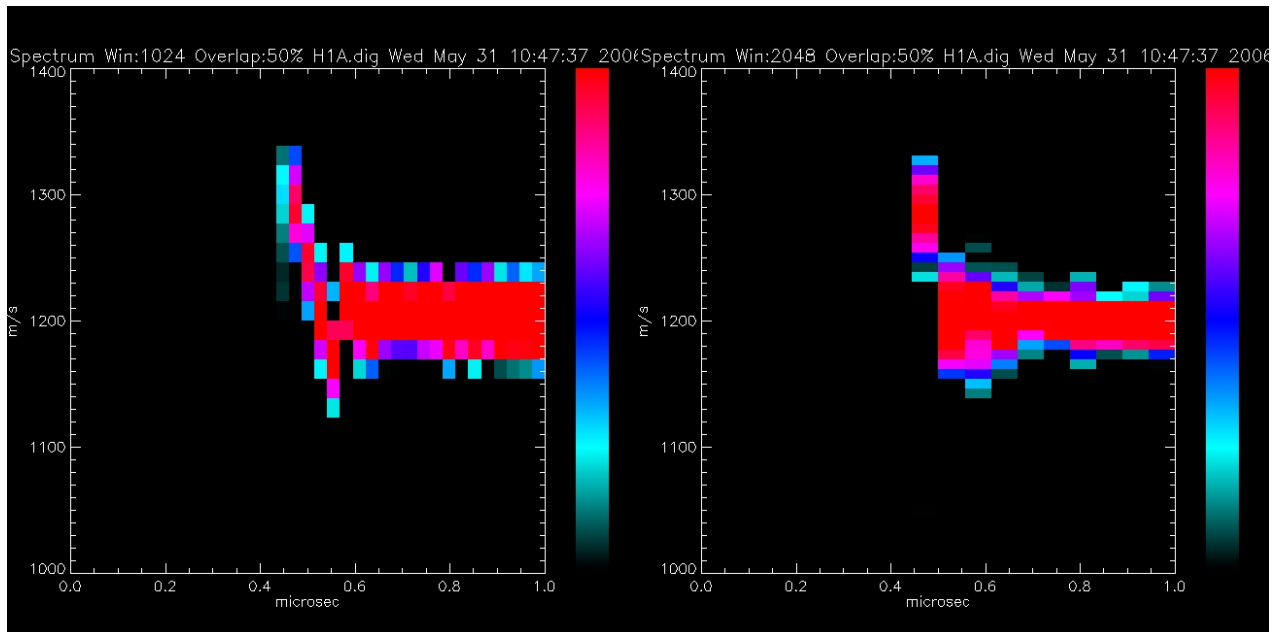


Figure 3: Expanded PDV Spectrograms. The left-hand diagram is purely an expansion of part of Figure 2, while the right-hand diagram uses an bin size of 2048 points. Notice the tradeoff between the greater time resolution on the left and the greater frequency resolution on the right. In both cases 20 dB of data are shown.

The region around shock breakout is expanded in Figure 3. The peak in velocity and subsequent pullback and ringing are clearly visible. In order to determine the peak stress accurately, we must measure the peak velocity (before any pullback). However, because the FFT process bins the data before calculating frequencies, there is an inherent tradeoff between time resolution and frequency resolution. The greater the binning in the time domain, the greater the frequency resolution. For frequencies which are not strongly time-dependent – such as the constant velocity achieved by the surface for several microseconds after spallation – this is not much of a limitation, and quite precise frequencies (and thus velocities) can be measured. In the region of time in which pullback occurs, however, the beat frequency is changing rapidly. Binning a number of points in the time domain has the effect of smearing these frequencies out in time. On the other hand, decreasing the binning to increase the temporal resolution – and thus isolating the peak frequency of pullback – lowers the accuracy to which the frequency can be determined.

In an attempt to quantify this effect and to determine the best parameters for extracting a reliable velocity from a PDV spectrogram, I measured peak positions and widths as a function of the FFT bin size. The results are shown below in Figure 4 (in frequency-space) and Figure 5 (where the frequencies have been converted to stress by the computer program *Impact*). In both cases the yellow shaded area shows the extent of the spectral peak (defined as the -3 dB point from the maximum) and the green lines show the peak itself. The blue line shows the velocity of the surface once it is constant. As expected, the precision of the frequency measurement increases with increasing bin size. However, the value of the measured frequency also changes. At large bin sizes, “contamination” with the asymptotic surface velocity overwhelms the signal from the actual

pullback region. As the binning decreases, the frequency increases, but the width of the peak (and thus the uncertainty in the frequency) also increases. As a result, the pullback frequency – and thus the peak stress state of the system – is difficult to determine to better than ± 50 MHz, which corresponds to a pressure uncertainty of ± 7 kbar for molybdenum. Varying the bin overlap from 1 % to 99 % did not improve this problem, nor did changing the window function from a Bartlett window to a Blackman-Harris, Hanning, or Welch window.

In principle the accuracy of the PDV system should be extremely high. It depends on three things – accurate time measurement by the digitizer, accurate wavelength output by the laser, and a high enough signal-to-noise ratio to measure the result. In the case of our experimental apparatus, the combined time and wavelength uncertainty is on the order of 0.02 %, and the signal-to-noise ratio was better than 40 dB in all but one case. The resolution bottleneck seems to reside in the analysis procedure. More advanced spectral decomposition techniques, such as wavelet-based methods or the Hilbert-Huang transformation, have the potential to ameliorate this problem.

Figure 4

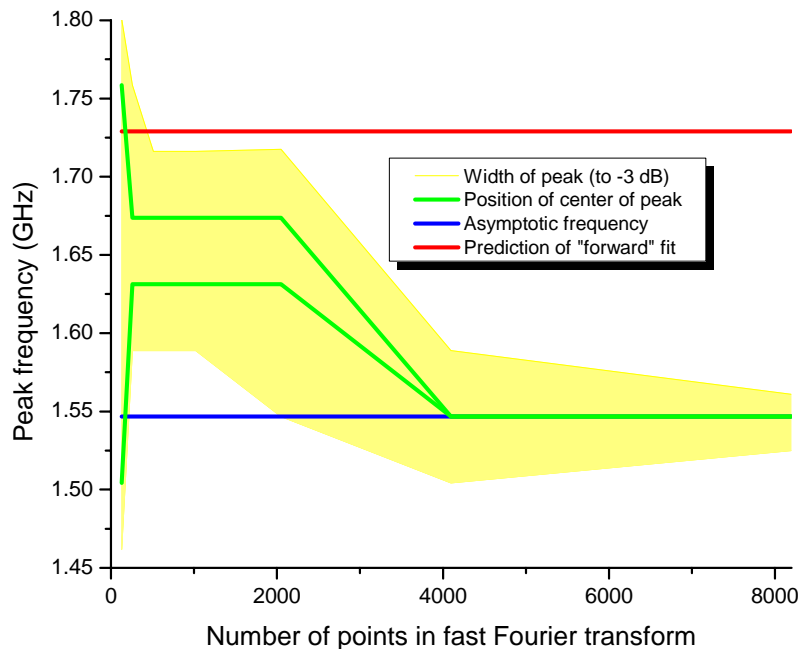


Figure 4: Measured peak frequency under different analysis conditions. This plot shows the peak frequency as a function of the number of data points used in the Fourier analysis. The analysis was performed with 50 % bin overlap and a Bartlett window. The data sets are explained in the text.

Figure 5

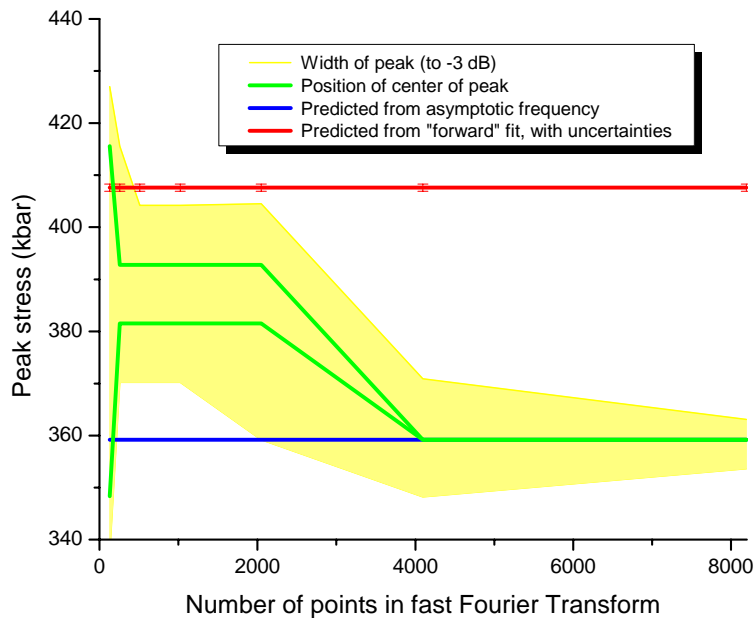


Figure 5: Calculated peak stress state under different analysis conditions. The analysis was performed as described in Figure 4, above.

As an alternative, however, I have pursued a different tack, modeling the data in the velocity domain and then transforming it forward into the time domain. This procedure relies on our prior knowledge of the expected velocity profile of the surface. We expect to see a discontinuous change in velocity from one constant value to another when a shock (or other wave) wave reaches the free surface. Pullback can be represented by an exponential decay in velocity, while the subsequent ringing in the spall scab resembles a damped sinusoidal oscillation. In the experiment, this surface motion is encoded by the PDV process into a time-domain signal. Instead of trying to reconstruct the surface motion by mathematical transformation of the PDV signal, I started with a velocity model, transformed it “forward” to the time domain by analytical inverse Fourier transform, and fit its parameters to the time-domain signal directly.

The implementation of this procedure is straightforward, though much more computationally demanding than Fourier transformation. The velocity model was defined as a sum of elements – Heaviside functions, exponential decays, and damped sine waves – with adjustable parameters. (See Table I.) The combined model was converted analytically to the time domain by inverse Fourier transform. The time-domain parameters were then adjusted to give the best fit to the data by a standard nonlinear least squares Levenberg-Marquardt method. (These calculations were performed using the *MATLAB Optimization Toolbox* from The Mathworks.) Fifteen adjustable parameters were used to fit the data between the start of the record and probe impact. The harmonics visible in the spectrogram could be fit using this model, though filtering the data before processing to remove frequency components between 1 MHz and 3 GHz was computationally more tractable.

The results of this analysis are compared to the FFT results in Figure 6, and are shown in comparison to the derived frequencies and pressures in Figures 4 and 5 as the red lines. The peak velocity of the pullback was determined to within ± 0.002 km/s (± 25 MHz), and thus the peak pressure was found to be 407.6 kbar ± 0.7 kbar. This is significantly more precise than the value found by examination of the FFT spectrogram. Its accuracy, though, is somewhat more difficult to determine, because the predicted velocity lies outside of the range of the peak found by FFT for bin sizes of 512 or more points. Comparison with an independent velocimetry method (such as VISAR) on a future experiment might help to resolve this question of accuracy.

This “forward” fitting method has some advantages over spectral decomposition techniques. First, it can have high time and frequency resolution simultaneously, because the two parameters can be varied independently. Second, it systematically seeks the best result and provides a quantitative measure of the uncertainty in its output. Third, features which are identical in several datasets can be fit together, improving the accuracy of the result. For example, the velocity caused by the precursor wave in molybdenum seemed to be independent of the thickness of the sample, so both precursor waves could be fit together. This improved the accuracy to which the velocity of this wave was determined by a factor of five. It would be somewhat more difficult to combine information across datasets systematically with spectral methods.

Figure 6

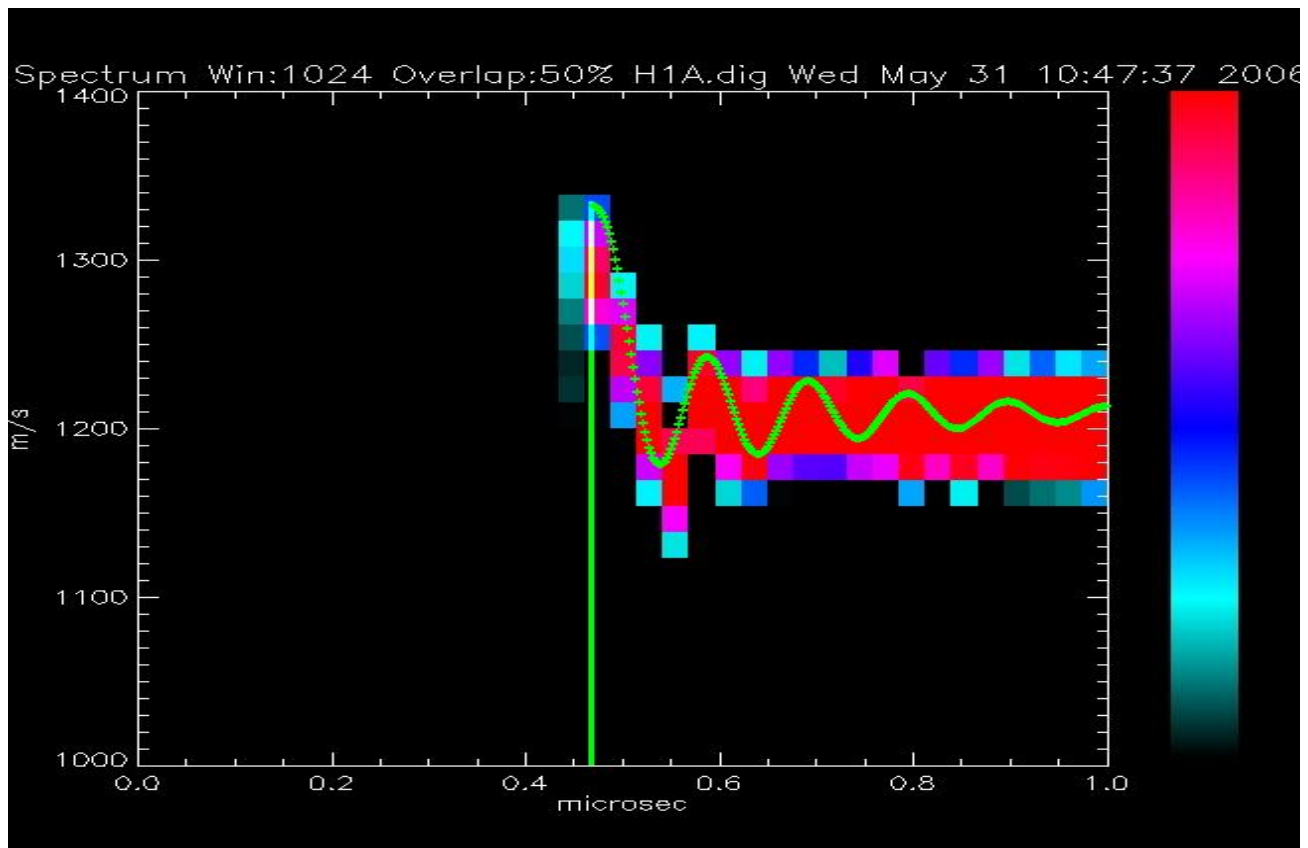


Figure 6: Expanded PDV Spectrogram Showing “Forward” Fit. This figure reproduces the left-hand part of Figure 3, with the results of the “forward” fit in this region overlain in green.

Table I: “Forward” Model Parameters

<u>Modeled Feature</u>	<u>Modeling Function</u>	<u>Adjustable Parameters</u>
Precursor wave	Heaviside function	Starting position (and phase in time domain), amplitude
Shock wave	Heaviside function	Starting position (and phase in time domain), amplitude
Pullback	Exponential decay	Starting position, amplitude, decay rate
Ringing	Damped sine wave	Starting position, amplitude, frequency, phase, decay rate
Probe impact	Heaviside function	Position (output forced to zero after this time)
Harmonics	All of above	Integer frequency multiple, amplitude (held constant over all harmonics)

Table II: Computation Times

<u>Method</u>	<u>Time Required</u>
FFT spectrogram	< 5 seconds
Forward fit, FFT results as initial guess, fit constant velocity only	30 minutes
Forward fit, as above fitting all components except harmonics	2 hours
Forward fit, as above fitting all components	5 hours
Full fit, as above with <i>a priori</i> initial guess	> 10 hours

Spectral methods retain two significant advantages over this “forward” fitting method. First, they make no assumptions about the form the data will take. Experiments which give unexpected results can still be analyzed by FFT, while a fitting procedure might fail or give meaningless results. Second, FFT-like methods are much more efficient computationally. Table II lists the time several calculations took on a 2 GHz Pentium laptop computer. There is most likely some room for code optimization, but the orders of magnitude of difference in computation time between the two

methods imply that spectral methods are much more appropriate for rapid data analysis. Ideally, the two methods could be used together – spectral methods could give an initial result and provide a starting point for a forward fit, which then would give a precise final answer (assuming that the accuracy question posed above were answered satisfactorily).

III. Predicted Shock Pressures in Tin

The large number of experiments done on this campaign allowed us to quantify the effect of sample thickness on the peak shock stress in tin. Figure 7, below, shows the peak stresses achieved for various combinations of sample thickness and explosive drive. The results were highly reproducible: the experiments at 2.5 mm and 3.5 mm of tin with PBX 9501 as the explosive were repeated, and the resulting peak stresses agreed to within the measurement uncertainties. The PBX 9501 shots all showed a pullback of approximately 5 kbar, while the Detasheet shots consistently gave one of 7 kbar. The PBX 9501 results were reasonably well-described by a quadratic relationship between stress and thickness; the small number of data points taken with a Detasheet drive made a quadratic fit exact but not necessarily predictive. These results could be used to guide future experiments involving explosively-driven tin.

Figure 7

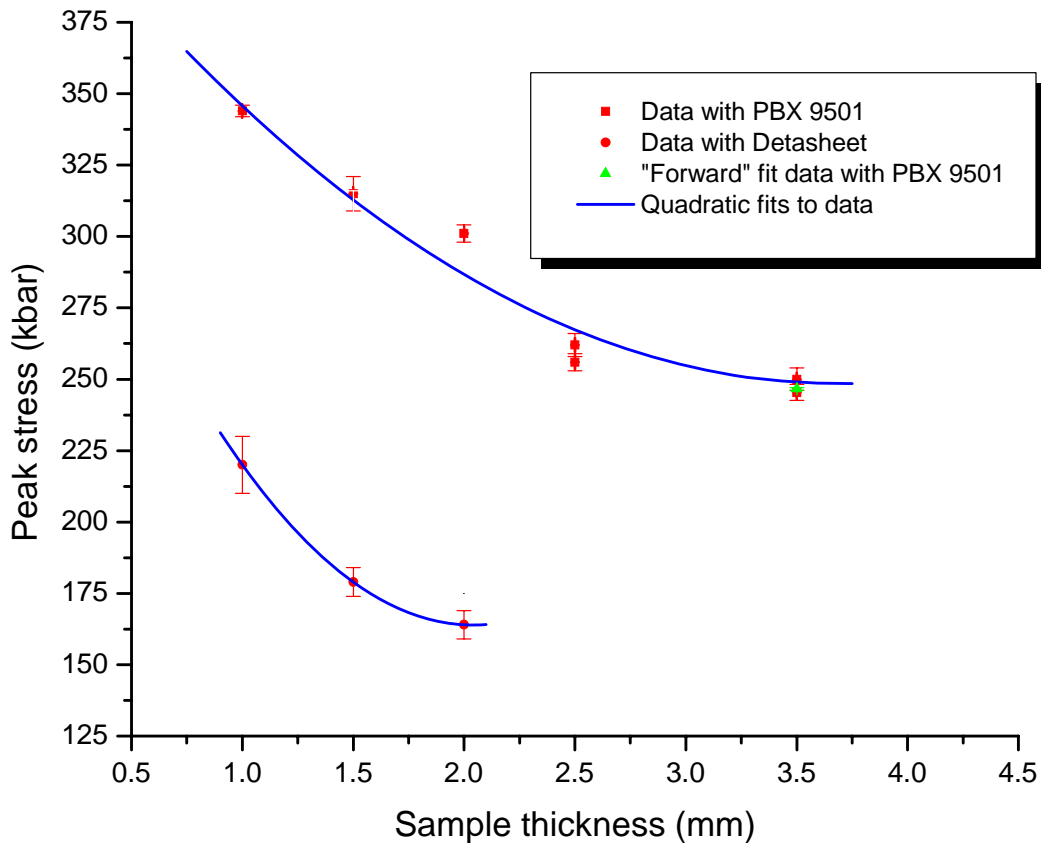


Figure 7: Peak stress as a function of sample thickness in explosively-driven tin. Peak stresses were determined by FFT, and their uncertainties reflect the frequency width of the pullback peak. “Forward” modeling of one experiment’s data gave uncertainties of less than 0.4 kilobar. The uncertainty in the sample thicknesses was ± 0.001 mm.

IV. Conclusions and Future Directions

The “forward” fitting method has great promise as a complement to spectral methods for PDV data analysis. Its accuracy for peak pressures must be verified – either by checking against an independent method of velocimetry or by further simulation with synthetic datasets. Assuming that it is indeed accurate, this method provides more precise measurements of many experimental observables. Increased computational efficiency would make it even more useful. Finally, our results for tin provide a guide for future experimenters who wish to vary peak stresses in explosively-driven experiments.

V. Acknowledgments

I would like to acknowledge the experimental collaboration of Mark Wilke, Steve Jaramillo, and Andrew Montoya of P-23, Achim Seifter of P-24, and Dale Turley, Jerry Stevens, Lynn Veaser, Adam Iverson, Sarah Giandoni, and Mike Grover of Bechtel Nevada. The funding for these experiments was provided by Campaign 2 and the Agnew Fellowship.

MRF:mrf

cc: P-23 File

H803	Billy Butler
H803	Dave D. Clark
H803	Anemarie Deyoung
H803	Steve Elliott
H803	Doug Fulton
H803	Michael Furlanetto
H803	Gary Grim
H803	Nick King
H803	Andi Klein
H803	Kris Kwiatkowski
H803	Steve Lamoreaux
H803	Kevin Morley
H803	Andy Obst
H803	Jeremy Payton
H803	Gus Sinnis
H803	Dan Sorenson
H803	Mark Wilke
H803	Michael Zellner
D410	Dave A. Clark
D410	Dave Holtkamp
E526	Dennis Paisley
E526	Achim Seifter
E526	Damian Swift
P952	Rob Hixson
P918	Dave Funk
H846	Chris Morris
H846	Dale Tupa
D434	Jack Shlachter
T085	Mark Potocki
P940	Matt Briggs
P940	Will Hemsing
P940	Mike Shinas
BN/STL	Bruce Marshall
BN/STL	Jerry Stevens
BN/STL	Dale Turley
BN/STL	Lynn Veaser
BN/LAO	Dave Esquibel
BN/LAO	Sarah Giandoni
BN/LAO	Tom Graves
BN/LAO	John Hollabaugh
BN/LAO	Adam Iverson
BN/LAO	Fred Sanders
BN/LAO	Tom Tunnel
LLNL	Ted Strand
SNL	Dan Dolen
SNL	Mike Furnish